Theor Chem Acc (1998) 100:204–211
DOI 10.1007/s002149800m42

Theoretical
Chemistry Accounts

Regular article

Ab initio quantum dynamical study of the vinylidene-acetylene isomerization*

R. Schork, H. Köppel

Theoretische Chemie, Physikalisch–Chemisches Institut, Universität Heidelberg, Im Neuenheimer Feld 253, D-69120 Heidelberg, Germany

Received: 5 June 1998 /Accepted: 23 July 1998 / Published online: 9 October 1998

Abstract. The dynamics of vinylidene-acetylene isomerization has been studied quantum mechanically, based on a new ab initio calculated potential energy surface (PES). The grid underlying the PES and the dynamic treatment rest on planar 4-atom Jacobi-like coordinates. Three degrees of freedom, the C—C bond length and the two Jacobi-like angles are treated explicitly, while the two other coordinates relating to the C—H bond lengths have been optimized in the ab initio treatment. The energies of the resulting 3D grid have been computed with the CCSD(T) method, using a cc-pVTZ basis set, while selected stationary points have been characterized at a higher level of theory. The subsequent dynamic treatment reproduces very satisfactorily the experimental photodetachment spectrum of Lineberger and coworkers. Preliminary results are also reported for the lifetime of vinylidene.

Keywords: Ab initio potential energy surface – Vinylidene – Photodetachment spectrum – Wavepacket propagation

1 Introduction

The vinylidene-acetylene isomerization reaction is a prototypical example of a 1,2-hydrogen shift [1]. This important type of unimolecular reaction often leads to the disappearance of small carbenes [2–4] and nitrenes [5, 6]. Also vinylidene itself is considered to be an important reactive intermediate in organic chemistry [7–10] and has been studied extensively, both experimentally [11–14] and theoretically [15–20]. We refer to these studies for further references on the subject.

Whether vinylidene exists at all and has a lifetime long enough to be observed by spectroscopic techniques remained a central question for a long time. The first theoretical estimates of the classical reaction barrier for the rearrangement yielded 6.4 [15] and 2.2 [16] kcal/mol. The effect of the zero point vibrational energy reduced these to 4.6 and 0.9 kcal/mol, respectively, implying that the activation energy might vanish. The question of the existence of this species was settled when Lineberger and coworkers [11, 13] observed vibrational states of vinylidene in the ultraviolet photoelectron spectrum of the stable vinylidene anion H_2CC^-. From the observed linewidths they deduced a strict lower limit for the lifetime of $\tau > 0.027$ ps. Moreover, the observation of excited vibrational levels in the rocking mode, representing the main reaction coordinate near the vinylidene minimum, shows that there must be a finite barrier for isomerization [13].

More recent theoretical studies confirmed the existence of vinylidene as a genuine minimum on the ground-state potential energy hypersurface of C_2H_2. Gallo et al. [17] performed CISD and CCSD calculations with various basis sets and estimated the classical barrier to be $\sim$3 kcal mol. Smith et al. [18] predicted a value of 2.6 kcal/mol using the QCISD(T) level of theory. They also reported an artificial intermediate minimum along the reaction path when using the MP2 method. Finally Chang et al. [19] performed extensive studies employing the CCSD(T) and CCSD(TQ) methods and correlation-consistent polarized valence basis sets (cc-pVXZ). The classical barrier, extrapolated to the full-CI and complete basis set limit, was found to be $\sim$2.85 kcal/mol [19].

The only dynamical calculation so far seems to be a semi-classical study by Carrington et al. [21] using a reaction path Hamiltonian. In this work a simple polynomial was used to approximate the potential energy along the reaction coordinate. Germann and Miller [22] have recently studied the importance of the vinylidene intermediate for the resonance tunneling in acetylene isomerization.

In the present work, we study the dynamics of the rearrangement of vinylidene using fully quantum mechanical methods, namely wavepacket propagation techniques. For this purpose a new 3D surface of the electronic ground state is calculated ab initio using the coupled cluster [CCSD(T)] [23, 24] method. An

* Dedicated to Prof. Dr. Wilfried Meyer on the occasion of his 60th birthday

Correspondence to: H. Köppel

additional smaller surface of the vinylidene anion is constructed which is used to generate a vibrational ground-state wavefunction of $C_2H_2^-$. This wavefunction is then transferred to the vinylidene surface to simulate the photodetachment spectrum of Ervin et al [13]. We obtain good overall agreement with the experimental spectrum, which is encouraging as regards the theoretical approach adopted. A further aim is to estimate the lifetimes of vinylidene and its metastable vibrational states. This is especially interesting as they have not been determined experimentally so far.

This paper is organized as follows. Section 2 describes the theoretical methods used. In the first part details of the electronic structure calculation are given, including results for the stationary points of the surface. The second part explains how the wavepacket has been propagated. In Sect. 3 further results of the ab initio calculation and results of the dynamical studies are presented and discussed. Finally, Sect. 4 concludes this paper with a short summary and an indication of future work.

2 Theoretical methodology

2.1 Electronic structure calculations

The grid of ab initio points to be calculated was essentially determined by the dynamical study to follow.

Planar 4-atom Jacobi-like coordinates as shown in Fig. 1 are a natural choice of coordinates. They are chosen here because the corresponding Hamiltonian [25, 26] has a simple form that is easy to implement within wavepacket propagation techniques. One coordinate is the C—C bond length R. The other four are polar coordinates $(r_1, \theta_1, r_2, \theta_2)$ of both hydrogen atoms with the origin X centered at the middle of the C—C bond. A sixth coordinate, describing out-of-plane motion, is not considered because all known stationary points of the system on the S_0 hypersurface are planar and stable with respect to out-of-plane distortion; therefore the reaction is expected to proceed through planar configurations throughout. We mention, however, that a non-planar transition state structure has been reported for triplet vinylidene [27].

The two polar angles θ_1 and θ_2 can be mixed to give the symmetric and asymmetric linear combinations θ_r and θ_s:

$$\theta_r = \theta_1 + \theta_2$$
$$\theta_s = 1/2\ (\theta_1 - \theta_2)$$

While θ_r corresponds to the rocking motion at the vinylidene minimum (both H-atoms moving in the same direction around the center), θ_s describes the scissor mode (with the H-atoms moving in opposite directions). The rocking mode is closest to the reaction coordinate near the vinylidene minimum.

Since a quantum dynamical calculation involving more than three degrees of freedom is cumbersome, we decided to build a 3D cartesian grid. The 3D grid selected consists of 600 points scanning the C—C bond length R and the two angular coordinates θ_r and θ_s. While the grid is equidistant in R and θ_r, it is denser in the central range of θ_s so as to correctly scan the finer features of the reaction path. For the smaller vinylidene anion surface mentioned below the same coordinates were used. Table 1 gives details of the regions covered by the grids for both the neutral and the anionic species.

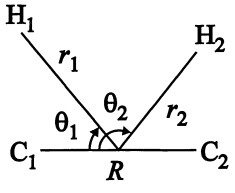

Fig. 1. Planar 4-atom coordinates used in the calculations

Table 1. Specification of the 3D grid used in the ab initio calculations

Coordinate	Number of points	Range
Vinylidene (neutral)		
θ_r	10	0–135 [deg]
θ_s	10	20–68 [deg]
R	6	2.25–2.60 [a.u.]
Vinylidene anion		
θ_r	3	0–30 [deg]
θ_s	4	24–48 [deg]
R	5	2.39–2.67 [a.u.]

At each of the above coordinate points two ab initio calculations were performed using Gaussian94 [28]. In a first step, the two X–H distances were optimized using the MP2 level of theory. Then the coupled-cluster method with single, double and a non-iterative inclusion of triple excitations [CCSD(T)] was used to determine the singlet ground state potential energy at that point. Both calculations use Dunning's correlation-consistent polarized valence triple-ζ basis set (cc-pVTZ) [29], resulting in 88 contracted Gaussian basis functions (156 primitive Gaussians). The calculations were performed at the High-Performance Computing Center Stuttgart on a NEC SX-4/36 Cluster. Each point of the vinylidene surface took 23 min of processing time on average. For the anion a similar, but smaller, grid was constructed which is centered at the $C_2H_2^-$ equilibrium conformation. It consists of 60 points that were calculated at the same level of theory; the processing time was about 54 min per point. Table 2 shows the geometries and energies of the stationary points at the given level of theory; these data have been obtained independently from an unconstrained (planar) geometry optimization. As regards neutral vinylidene the table reproduces earlier results of Ref. [19]. We also refer to this work for a discussion of these results and a comparison with the considerable amount of earlier literature. For the vinylidene anion, our results are generally in line with previous calculations [13, 30, 31], but the C—C distance comes out somewhat smaller than in the earlier work.

2.2 Wavepacket dynamical calculations

As already stated, the dynamical calculations were performed using the same 4-atom Jacobi-like coordinates as in the ab initio studies. The evolution in time of a wavepacket is thus defined by the following Hamiltonian in which the kinetic energy has a particularly simple form [25, 26, 32]:

$$\hat{H} = \hat{H}_R + \hat{H}_\theta + \hat{V}_{\text{eff}} + \hat{V} \tag{1}$$

$$\hat{H}_R = -\frac{\hbar^2}{2m}\frac{\partial^2}{\partial r_1^2} - \frac{\hbar^2}{2m}\frac{\partial^2}{\partial r_2^2} - \frac{\hbar^2}{2M}\frac{\partial^2}{\partial R^2} \tag{2}$$

$$\begin{aligned}\hat{H}_\theta = &-\frac{\hbar^2}{2}\left[\frac{1}{m}\left(\frac{1}{r_1^2}+\frac{1}{r_2^2}\right)+\frac{4}{M}\frac{1}{R^2}\right]\frac{\partial^2}{\partial\theta_r^2}\\ &-\frac{\hbar^2}{8m}\left(\frac{1}{r_1^2}+\frac{1}{r_2^2}\right)\frac{\partial^2}{\partial\theta_s^2}\\ &-\frac{\hbar^2}{2m}\left(\frac{1}{r_1^2}-\frac{1}{r_2^2}\right)\frac{\partial^2}{\partial\theta_s\theta_r},\end{aligned} \tag{3}$$

$$\hat{V}_{\text{eff}} = \frac{-\hbar^2}{8}\left(\frac{1}{mr_1^2}+\frac{1}{mr_2^2}+\frac{1}{MR^2}\right) \tag{4}$$

$$\frac{1}{M} = \frac{2}{m_C}, \quad \frac{1}{m} = \frac{1}{m_H} + \frac{1}{m_H + 2m_C}\ .$$

In the derivation of these equations a minor approximation (neglect of an off-diagonal term) which introduces an error that is estimated to be a few percent [25] is used. Additionally, the wavefunction is

Table 2. Optimized geometries and energetics for the stationary points of the vinylidene-acetylene system (bond distances in Å, angles in deg.)

Stationary point	C_1—C_2	H_1—C_1	H_2—C_1	$\angle H_1C_1C_2$	$\angle C_2C_1H_2$	Energy [Hartree]	ΔE [kcal/mol]
Vinylidene	1.301	1.081	1.081	120.00	120.00	−77.145149	0.0
Transition state	1.255	1.379	1.067	53.78	178.33	−77.141435	2.33
Acetylene	1.206	2.265	1.059	0.00	180.00	−77.218312	−45.91
Vinylidene anion	1.341	1.104	1.104	124.06	124.06	−77.148419	−2.05

scaled by a factor of $(Rr_1r_2)^{1/2}$, leading to the effective potential part (Eq. 4) of the Hamiltonian.

In our 3D calculations, only the terms acting on the θ_r, θ_s and R coordinates were considered. Unless otherwise stated, the distances r_1 and r_2 appearing in these terms were set to values that match the vinylidene geometry ($r_1 = r_2 = 1.515$ Å). The grid calculated by ab initio methods is too coarse for dynamical calculations and does not cover the full range of momenta that is relevant to our study. Instead of performing more ab initio calculations, additional points were determined by interpolation. To interpolate the base grid, one-dimensional cubic splines were used iteratively as suggested in [33]. As the grid does not cover the asymptotic areas of the potential surface, no special boundary conditions are available. Instead, the "not-a-knot" conditions suggested by de Boor [34] are used. For the production calculations, a grid of $64(\theta_r) \times 64(\theta_s) \times 16(R)$ points has been employed. A fast Fourier transform (FFT) scheme [35] is used to calculate the action of the Hamiltonian on the time-dependent wavefunction represented on this grid.

During the propagation, parts of the wavefunction cross the potential barrier and wander towards the acetylene stationary point. This region is not included fully in the grid of ab initio points; rather the latter ends shortly behind the barrier. Therefore, care has to be taken to prevent the wavefunction from hitting the boundary as this would cause artificial reflections (or reappearence on the other side of the grid if FFT methods are used to evaluate the Hamiltonian). This goal is accomplished by introducing a complex absorbing potential (CAP) [36–38] which removes the wavefunction that has passed the barrier. The CAP is zero everywhere except behind the energy barrier, where it grows rapidly:

$$V_{\mathrm{CAP}}(x) = \begin{cases} 0 & x \le x_0 \\ -i\eta(x - x_0)^3 & x > x_0 \end{cases} \tag{5}$$

Here x is a linear combination of θ_r and θ_s and points towards the direction of the reaction path. The coefficient η sets the strength of the CAP. It has to be chosen to minimize both transmission through and reflection back from the CAP and depends on the kinetic energy of the wavepacket. While this choice can be difficult in general, it seems to be much easier here because the given potential decreases strongly in the area of interest. This reduces the probability of a reflection even when a relatively strong CAP is used. In the calculation reported below, a value $\eta = 0.002$ (a.u./rad^3) was found satisfactory for these purposes.

To propagate the wavefunction in time, the Lanczos-Arnoldi algorithm [39, 40], a variant of the short iterative Lanczos (SIL) algorithm [41], was used. The Lanczos-Arnoldi scheme has to be used because SIL works only with a hermitian Hamiltonian; this prohibits the use of a CAP.

The spectrum is calculated by a FFT of the autocorrelation function

$$C(t) = \langle \psi(0) | \psi(t) \rangle. \tag{6}$$

To simulate a photodetachment spectrum, $|\psi(0)\rangle$ in Eq. (6) is identified with the ground vibrational wavefunction of the vinylidene anion (H_2CC^-) placed on the vinylidene S_0 potential surface. This models a vertical (Franck-Condon) transition as is justified by the fast asymptotic velocity of the ejected electron (about 10 Å/fs) [13]. The ground state wavefunction is determined by propagating an approximate wavefunction in imaginary time on the small anion potential energy surface (PES) described in Sect. 2.1. This successively reduces the norm of the higher-energy components of the initial wavefunction so that finally only the component with the lowest energy – the ground state – remains.

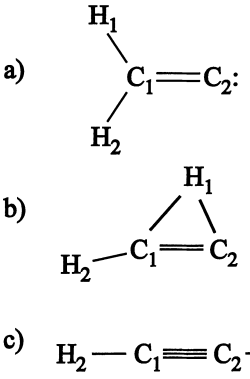

Fig. 2. The stationary points of the vinylidene-acetylene rearrangement process

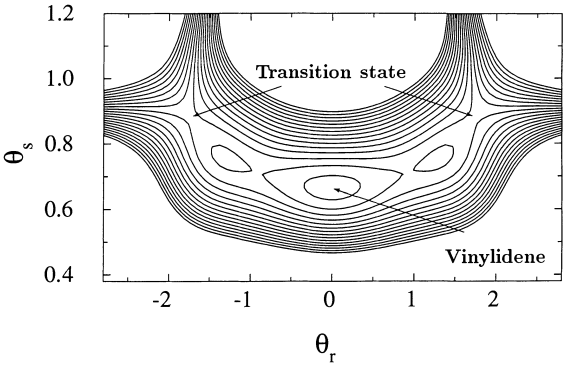

Fig. 3. 2D-plot of the S_0 potential energy surface. The third coordinate R is optimized at each point (angles in rad). Neighboring contour lines indicate an energy difference of 1 kcal/mol, with the innermost contour being located at an energy of 1 kcal/mol above the vinylidene local minimum

The wavepacket propagation scheme also allows determination of the eigenfunction associated with a given resonance by spectral quantization [42, 43]. This method extracts the eigenfunction $\psi_v(x)$ by a Fourier transform of the time-dependent wavefunction at a peak frequency ω_v of the spectrum:

$$\psi_v(x) \sim \int_{-\infty}^{\infty} \langle x | \psi(t) \rangle \mathrm{e}^{i\omega_v t} dt. \tag{7}$$

The eigenfunction can then be analyzed, e.g. to check the assignment of the spectral peaks to vibronic transitions.

3 Results and discussion

3.1 Analysis of the PES

Figure 3 shows a 2D contour line drawing of the new PES where the C—C bond length R is optimized at each

Table 3. Optimized geometries for the secondary transition and minimum structure found (bond distances in Å, angles in deg.)

Stationary point	C_1—C_2	H_1—C_1	H_2—C_1	$\angle H_1C_1C_2$	$\angle C_2C_1H_2$
Sec. transition struct. (cc-pVTZ)	1.278	1.132	1.067	81.51	156.71
Sec. minimum (cc-pVTZ)	1.267	1.185	1.067	67.71	170.49
Sec. minimum (cc-pVQZ)	1.265	1.187	1.069	67.78	170.69

point. The minimum in the center corresponds to the vinylidene stationary point. To the left and right, the reaction path leads to the energy barrier associated with the transition state; this represents the possibility of either H_1 or H_2 moving around the molecule towards the second C-atom (C_2 in Fig. 2). Behind the energy barrier, there is a strong lowering of the potential energy towards the acetylene global minimum which is not included in the figure.

An unexpected feature of the PES is a shallow secondary minimum along the reaction path from vinylidene towards the transition state. A similar, though much deeper, minimum was reported in Ref. [18] for an MP2 PES. Since it disappeared in higher-level calculations (MP4 and QCISD), it was considered an artifact of the MP2 procedure.

To check if this minimum is a result of the interpolation of our discrete grid of ab initio data points, further optimization calculations at the CCSD(T)/cc-pVTZ level of theory were done with no other restriction on the coordinates than planarity. Indeed, the secondary minimum and a secondary transition state separating it from the vinylidene minimum were found at the expected locations; a subsequent frequency calculation confirmed that the minimum has no imaginary frequencies. The resulting geometries are given in Table 3. Additionally, to improve our calculations further, the energies of these stationary points were recalculated with the cc-pVQZ basis set and full optimization of the secondary minimum with this bigger basis set was done; the geometry thus determined is also included in Table 3.

The energies of the stationary points are presented in Table 4. The secondary minimum is very shallow, the barrier towards vinylidene being only 0.23 kcal/mol. Use of the cc-pVQZ basis set reduces the depth of this minimum to 0.16 kcal/mol. It does not seem likely that the minimum will disappear as one approaches the complete basis set limit. However, an improved treatment of the correlation energy [e.g. CCSDT or CCSD(TQ)] might very well remove it. A similar minimum on the MP2 surface mentioned above has a slightly different geometry [$r(H_1—C_1 = 1.202$ Å, $r(C—C) = 1.273$ Å]. The well depth is reported to be 0.48 kcal/mol with the 6-311G(d,p) basis set and even increases when the basis set is enlarged [18].

3.2 Photodetachment spectrum

The simulated photodetachment spectrum of our 3D dynamical calculation is compared with the experimental spectrum of Ervin et al. [13] in Fig. 4. The overall agreement with our simulated spectrum using purely ab initio data is fairly good. Starting from the right and following the 0-0 line, one can see two weak transitions of the CH_2 rocking mode (two and four quanta). The frequency of the 2←0 rock transition is 366 cm^{-1}; this differs from the (larger) experimental value by about 80 cm^{-1} as shown in Table 5. In our simulated spectrum the 4←0 rock transition has a higher intensity than the 2←0 transition, while it is barely visible in the experimental spectrum. We ascribe this to the secondary minimum reported in Sect. 3.1, which strongly changes the wavefunctions of these eigenstates and thus the overlaps with the anionic ground-state wavefunction (see below). If this is true, the absence of this line in the experimental spectrum means that the secondary minimum is indeed an artifact of the ab initio method used.

Table 4. Relative energies of the CCSD(T)/cc-pVTZ optimized stationary points, calculated with the cc-pVTZ and cc-pVQZ basis sets (in kcal/mol)

Stationary point	ΔE (cc-pVTZ)	ΔE (cc-pVQZ)
Vinylidene	0.0[a]	0.0[b]
Sec. transition structure	1.45	1.46
Sec. minimum	1.22	1.30[d]
Transition structure	2.33	2.41[c]

[a] Absolute energy $E = -77.145149$ [Hartree]
[b] Absolute energy $E = -77.194535$ [Hartree][c]
[c] Taken from Ref. [19]
[d] Same result as with cc-pVQZ optimized geometry

The remaining intense lines are the 1←0 CH_2 scissor and the 1←0 C—C stretch transition. The frequency of the CH_2 scissor mode is 1289 cm^{-1} which differs from the experimental value by about 120 cm^{-1}. The C—C stretch mode has a frequency of 1633 cm^{-1}; this is in very good agreement with experiment. Here one has to consider that the coordinate R, the C—C distance, almost perfectly matches the coordinate of the C—C stretch normal mode. The same is only approximately true for θ_r and θ_s which, aside from the rock and scissor mode, also include a small mixed-in component of the C—H stretch modes. The relative intensities of these two symmetric modes are very well described by theory.

To check the assignment of the lines in the spectrum, spectral quantization was used to calculate the eigenfunctions corresponding to the dominant transitions. As indicated in Sect. 2.2 the eigenfunctions are determined from the time-dependent wavepacket. Snapshots of the latter, for different propagation times, are shown in Fig. 5. The movement toward and beyond the barrier as well as the vibration in the scissor mode (period ~26 fs) can be seen clearly. In Fig. 6 the eigenfunctions of the ground state and the lowest three vibrationally excited

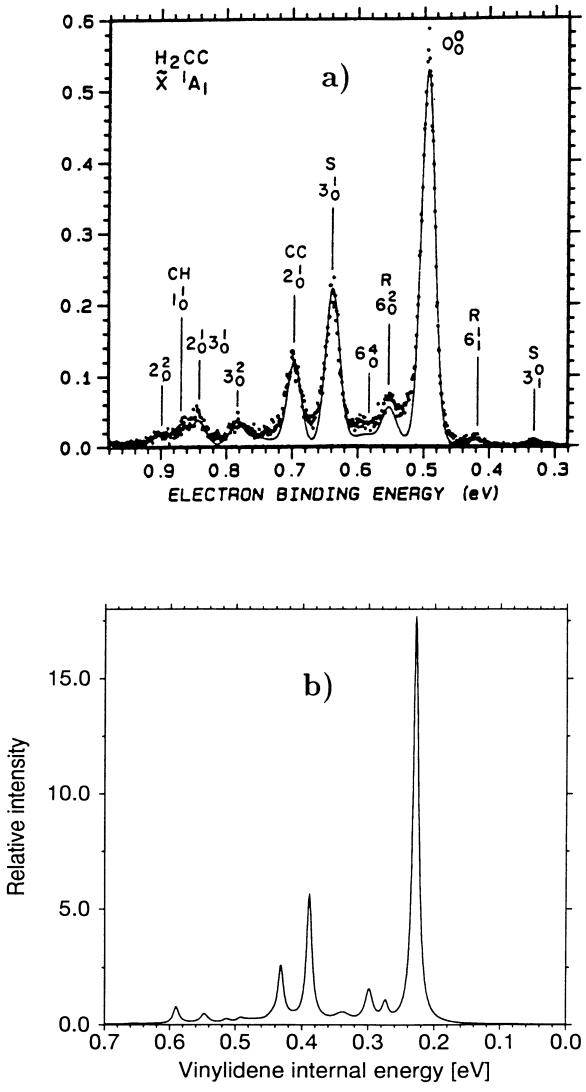

Fig. 4. **a** Experimental [13] and **b** simulated photodetachment spectrum of vinylidene in its $^1A_1$ singlet ground state. In **a** the actual measurement is represented by *dots*, while the *solid line* results from a Franck-Condon simulation

Table 5. Selected H_2CC vibrational frequencies (in cm^{-1})

Method	C—C stretch	CH_2 scissor	CH_2 rock (2 quanta)
Experimental[a]	1635 ± 10	1165 ± 10	450 ± 30
CCSD(T)/cc-pVTZ (harmonic)	1682	1234	646
Dynamic calculation (anharmonic)	1633	1289	366

[a] Taken from Ref. [13]

states are shown. Both the time-dependent wavepacket and the eigenfunctions in these figures result from a 2D calculation with fixed C—C bond length, but they do not change substantially in the 3D treatment, when the C—C bond length is allowed to vary. The ground state wavefunction is shown in Fig. 6a and vibrational wavefunctions with excitation energies of 366, 561 and 1289 cm^{-1} are shown in Fig. 6b–d. The latter clearly

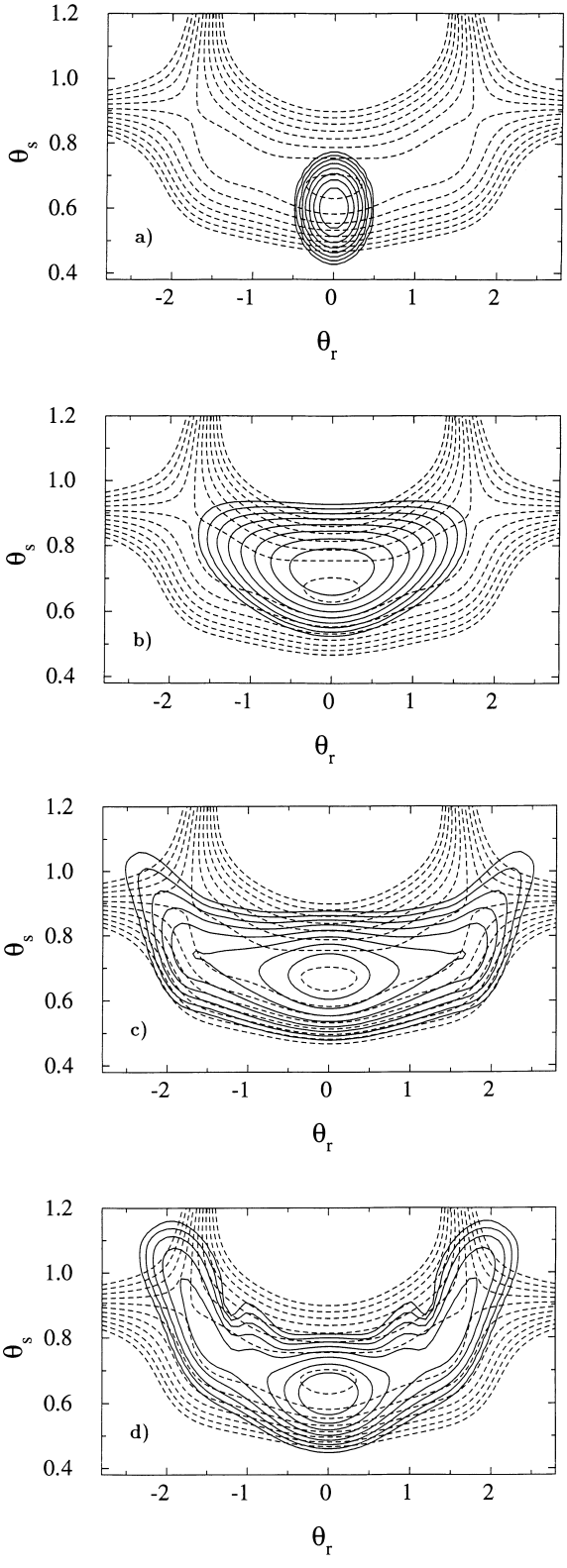

Fig. 5. 2D wavefunction at **a** time zero and after **b** 16 fs, **c** 32 fs and **d** 48 fs propagation time. The wavefunctions are plotted on a logarithmic scale; three contour lines mean a decrease by a factor of 10 in probability density

display the nodal pattern with two and four quanta in the rocking mode and one quantum in the scissor mode,

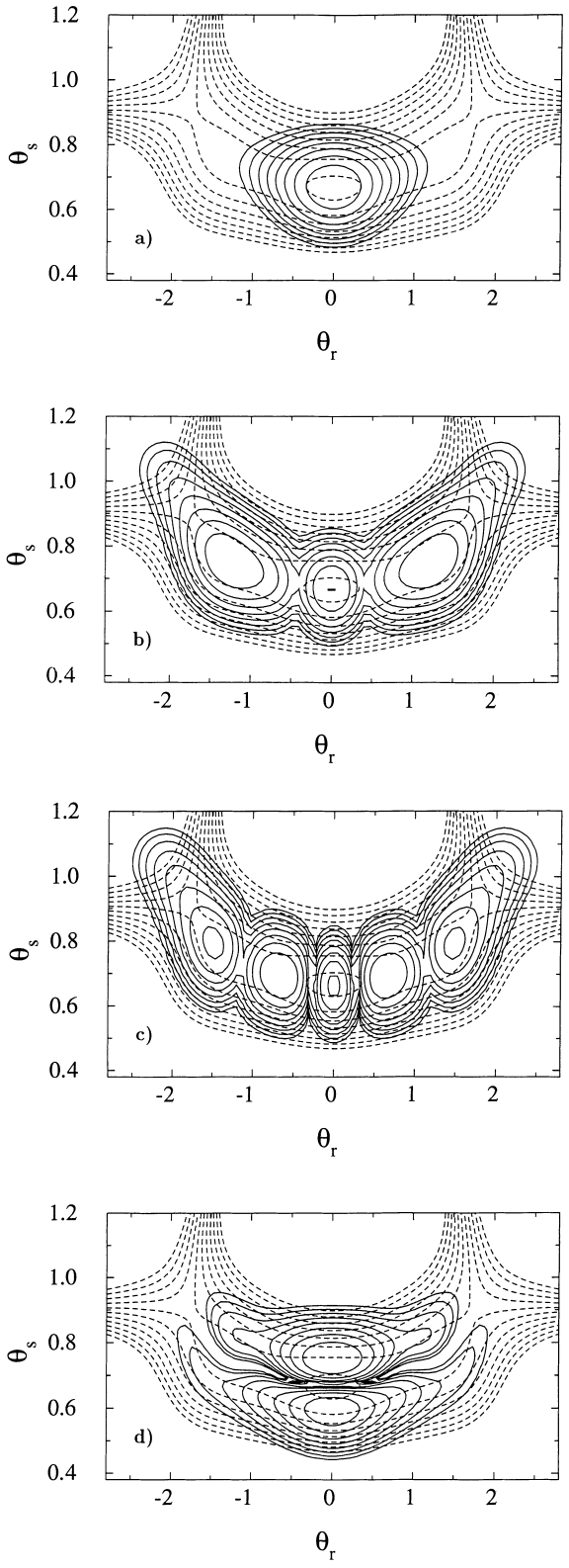

Fig. 6. 2D eigenfunctions of vinylidene. The wavefunctions are plotted on a logarithmic scale; three contour lines mean a decrease by a factor of 10 in probability density

repectively. This analysis fully supports the assignments discussed above and is consistent with the assignments of Ervin et al. [13] for their experimental spectrum.

3.3 Lifetime considerations

The decrease of the total norm of the wavefunction during a propagation time of 1024 fs is shown in Fig. 7. This decay is caused by the action of the CAP at the grid boundaries. Since the grid ends shortly behind the transition structure for the isomerization, the norm can also be interpreted as the survival probability in the vinylidene shallow well. This function is not a simple exponential function. Instead, at least three time regimes can be distinguished. In the first interval (~30 fs) the system propagates in the vinylidene local minimum without reaching the barrier. In the second time interval (from ~30 to 90 fs) there is a rapid decrease, characterized by a time constant of ~200 fs. Later on the decay becomes much slower. This indicates that the lifetime of vinylidene is very mode-specific. The fast decaying components probably correspond to the excited states, especially of the rocking mode. Figure 6 shows that these eigenfunctions have a bigger probability density near the barrier, implying a faster rate for isomerization. On the other hand, the vibronic ground state decays much slower, having a lifetime above 1 ps. In fact, in our present calculation the ground state even seems to "live" longer than 10 ps.

However, the present 3D treatment suffers from two shortcomings which may affect the computed lifetimes significantly. First, corrections due to the zero-point energy of the two C—H stretching modes as well as of the out-of-plane bending mode are not included in the calculation. From the known harmonic frequencies [17, 19] these are estimated to lower the activation energy by $\sim 250\,\mathrm{cm}^{-1}$, i.e. about 30% . Second, the C—H distance of the migrating hydrogen atom varies considerably during isomerization, leading to a corresponding change of the moments of inertia in the Hamiltonian (Eq. 1). This is not taken into account in the present work.

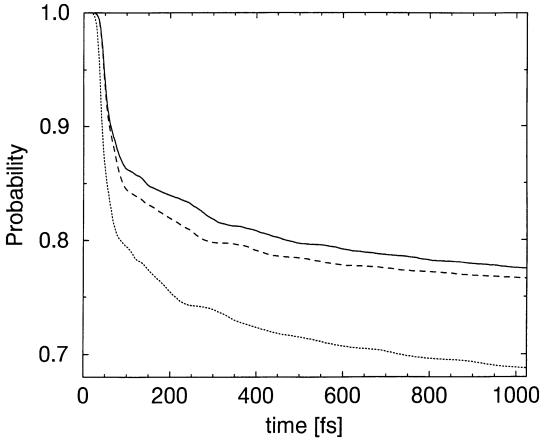

Fig. 7. Survival probability of the wavepacket, generated by the photodetachment process, in the vinylidene shallow well. The decrease of total norm of the wavefunction (3D calculation) is shown as a *solid line*. The *dashed line* represents the results of a 2D treatment, with the C—C bond length fixed and the coordinates r_1 and r_2 assigned the vinylidene value. The *dotted line* results from a 3D treatment where one of the coordinates r_1, r_2 is assigned its value at the transition state

Clearly, both corrections will affect the lifetime results considerably (more than the photodetachment spectrum which is determined by the nuclear motion near the vinylidene minimum). To get a preliminary idea about the second effect mentioned above, we have judiciously replaced one of the X—H distances in Eq. (3) by its value at the transition state ($r_1 = 1.128$ Å). The result for the survival probability is included in Fig. 7 and is seen to decrease considerably faster than before (cf. dotted with full line). This is easy to understand since at the saddle point the X—H distance is smaller than at the minimum ($r_1 = 1.515$ Å) amounting to a smaller effective mass. Of course the zero-point correction will have a similar effect and decrease the lifetime further. For further comparison, Fig. 7 also contains the result of a 2D treatment, with the C—C bond length fixed and the coordinates r_1 and r_2 again assigned the vinylidene value. This documents that the C—C stretching mode, although important in the photodetachment spectrum, has only a minor influence on the vinylidene lifetime. The small decrease in population caused by its suppression is probably connected with the reduced energy flow into modes different from the rocking mode, i.e. less competition with direct isomerization.

We mention that in the recent studies by Germann and Miller [22] on the isotopic scrambling of acetylene through the vinylidene intermediate some sharp resonances in the appropriate energy range also appeared. However, since quite different PESs were used, these data cannot be directly compared to ours.

4 Concluding remarks

In this study a 3D ab initio PES of the vinylidene-acetylene system was calculated using the CCSD(T)/cc-pVTZ level of theory. A secondary minimum on the reaction path from vinylidene towards acetylene that had only been documented before on an MP2 surface and was not expected to appear when using more elaborate methods was found. The nuclear dynamics on this new PES has been studied using wavepacket propagation techniques. The experimental photodetachment spectrum of Ervin et al. could be nicely reproduced, with the exception of an overly strong excitation of the rocking mode in the calculation. We take this as an indication that the aforementioned very shallow secondary minimum is probably an artifact of the present PES.

The survival probability of the wavepacket in the vinylidene shallow well, obtained in parallel, reveals a highly non-exponential behavior with a fast decay component of approximately 200 fs and another part decaying much more slowly, i. e. in the picosecond time range. Various ways have been indicated above for how to improve the dynamical treatment and thus determine the latter part more quantitatively. Another improvement would be, of course, to treat the C—H stretching coordinates as dynamical variables. Furthermore, a recalculation of the PES at a higher level of theory might be appropriate. Work along some of these lines is currently in progress in our group. In this way we hope to arrive at a reliable lifetime estimate for this important reactive intermediate.

Acknowledgements. The authors gratefully acknowledge financial support by the Deutsche Forschungsgemeinschaft through the Schwerpunktprogramm "Zeitabhängige Phänomene und Methoden in Quantensystemen der Physik und Chemie". Computer time has been generously provided by the Höchstleistungsrechenzentrum at the University of Stuttgart. We thank Prof. W.H. Miller for communicating results prior to publication. Special thanks go to Prof. C. Lineberger and colleagues for their kind hospitality and stimulating discussions which were essential to this project.

References

1. Schaefer HF III (1979) Acc Chem Res 12:288
2. Skell PS, Fagone FA, Klabunde KJ (1972) J Am Chem Soc 94: 7862
3. Reiser C, Steinfeld JI (1979) J Phys Chem 84: 680
4. Reiser C, Lussier FM, Jensen CC, Steinfeld JI (1979) J Am Chem Soc 101: 350
5. Travers MJ, Cowles DC, Clifford EP, Ellison GB (1992) J Am Chem Soc 114: 8699
6. Richards C, Meredith C, Kim SJ, Quelch GE, Schaefer HF III (1994) J Chem Phys 100: 481
7. Skell PS, Plonka JH (1970) J Am Chem Soc 92: 5620
8. Davison P, Frey HM, Walsh R (1985) Chem Phys Lett 120: 227
9. Dúran RP, Amorebieta VT, Colussi AJ (1987) J Am Chem Soc 109: 3154
10. Kiefer JH, Mitchell KI, Kern RD, Yong JN (1988) J Phys Chem 92: 677
11. Burnett SM, Stevens AE, Feigerle CS, Lineberger WC (1983) Chem Phys Lett 100: 124
12. Chen Y, Jonas DM, Kinsley JL, Field RW (1989) J Chem Phys 91: 3976
13. Ervin KM, Ho J, Lineberger WC (1989) J Chem Phys 91: 5974
14. Ervin KM, Gronert S, Barlow SE, Gilles MK, Harrison AG, Bierbaum VM, DePuy CH, Lineberger WC, Ellison GB (1990) J Am Chem Soc 112: 5750
15. Osamura Y, Schaefer HF III, Gray SK, Miller WH (1981) J Am Chem Soc 103: 1904
16. Krishnan R, Frisch MJ, Pople JA (1981) Chem Phys Lett 79: 408
17. Gallo MM, Hamilton TP, Schaefer HF III (1990) J Am Chem Soc 112: 8714
18. Smith BJ, Smernik R, Radom L (1992) Chem Phys Lett 188: 589
19. Chang N, Shen M, Yu C (1997) J Chem Phys 106: 3237
20. Chen W, Yu C (1997) Chem Phys Lett 277: 245
21. Carrington T Jr, Hubbard LM, Schaefer HF III, Miller WH (1984) J Chem Phys 80: 4347
22. Germann TC, Miller WH (1998) J Chem Phys 109: 94
23. Urban M, Noga J, Cole SJ, Bartlett RJ (1985) J Chem Phys 83: 4041
24. Raghavachari K, Trucks GW, Pople JA, Head-Gordon M (1989) Chem Phys Lett 157: 479
25. Bentley JA, Wyatt RE, Menou M, Leforestier C (1992) J Chem Phys 97: 4255
26. Sibert EL, Mayrhofer RC (1993) J Chem Phys 99: 937
27. Conrad MP, Schaefer HF III (1978) J Am Chem Soc 100: 7820
28. Frisch MJ, Trucks GW, Schlegel HB, Gill PMW, Johnson BG, Robb MA, Cheeseman JR, Keith T, Petersson GA, Montgomery JA, Raghavachari K, Al-Laham MA, Zakrzewski VG, Ortiz JV, Foresman JB, Cioslowski J, Stefanov BB, Nanayakkara A, Challacombe M, Peng CY, Ayala PY, Chen W, Wong MW, Andres JL, Replogle ES, Gomperts R, Martin RL, Fox DJ, Binkley JS, Defrees DJ, Baker J, Stewart JP, Head-Gordon M, Gonzalez C, Pople JA, (1995) Gaussian 94, revision D.3. Gaussian, Pittsburgh, Pa

29. Dunning TH (1989) J Chem Phys 90: 1007
30. Rosmus P, Botschwina P, Maier JP (1981) Chem Phys Lett 84: 71
31. Frenking G (1983) Chem Phys Lett 100: 484
32. Kolos W, Wolniewicz L (1963) Rev Mod Phys 35: 473
33. Press WH, Teukolsky SA, Vetterling WT, Flannery BP (1992) Numerical recipes in C: the art of scientific computing. Cambridge University Press, Cambridge
34. De Boor C (1978) A practical guide to splines. Springer Berlin Heidelberg New York
35. Kosloff D, Kosloff R (1983) J Comput Phys 52: 35
36. Neuhauser D, Baer M (1989) J Chem Phys 90: 4351
37. Vibók A, Balint-Kurti GG (1992) J Phys Chem 96: 8712
38. Riss UV, Meyer H.-D (1996) J Chem Phys 105: 1409
39. Arnoldi WE (1951) Q Appl Math 9: 17
40. Saad Y (1980) Lin Alg Appl 24: 269
41. Park TJ, Light JC (1986) J Chem Phys 85: 5870
42. Feit MD, Fleck JA Jr, Steiger A (1982) J Comput Phys 47: 412
43. Sadeghi R, Skodje RT (1993) J Chem Phys 99: 5126